Chinese Science Bulletin

ARTICLES

Validating global hydrological models by ground and space gravimetry

ZHOU JiangCun[1,2,3†], SUN HePing[1,2] & XU JianQiao[1,2]

[1] Institute of Geodesy and Geophysics, Chinese Academy of Sciences, Wuhan 430077, China;
[2] Key Laboratory of dynamic geodesy, Chinese Academy of Sciences, Wuhan 430077, China;
[3] Graduate University of Chinese Academy of Sciences, Beijing 100049, China

The long-term continuous gravity observations obtained by the superconducting gravimeters (SG) at seven globally-distributed stations are comprehensively analyzed. After removing the signals related to the Earth's tides and variations in the Earth's rotation, the gravity residuals are used to describe the seasonal fluctuations in gravity field. Meanwhile, the gravity changes due to the air pressure loading are theoretically modeled from the measurements of the local air pressure, and those due to land water and nontidal ocean loading are also calculated according to the corresponding numerical models. The numerical results show that the gravity changes due to both the air pressure and land water loading are as large as 100×10^{-9} m s^{-2} in magnitude, and about 10×10^{-9} m s^{-2} for those due to the nontidal ocean loading in the coastal area. On the other hand, the monthly-averaged gravity variations over the area surrounding the stations are derived from the spherical harmonic coefficients of the GRACE-recovered gravity fields, by using Gaussian smoothing technique in which the radius is set to be 600 km. Compared the land water induced gravity variations, the SG observations after removal of tides, polar motion effects, air pressure and nontidal ocean loading effects and the GRACE-derived gravity variations with each other, it is inferred that both the ground- and space-based gravity observations can effectively detect the seasonal gravity variations with a magnitude of 100×10^{-9} m s^{-2} induced by the land water loading. This implies that high precision gravimetry is an effective technique to validate the reliabilities of the hydrological models.

temporal variation of gravity field, Global Geodynamics Project, superconducting gravimeter, GRACE satellite gravity, global hydrological model

GEOPHYSICS

Global water cycle is an important mass migration phenomenon which is highly related to the human being's environment. The loading effects induced by transportation of water mass result in changes in various geophysical processes, e.g., Earth rotation, vertical land displacement, gravity fields, etc. Generally, the mentioned changes have seasonal or annual and semi-annual behaviors. Studies of Zhang et al.[1] and Zhang et al.[2] demonstrated that there exist obvious annual land water loading effects in the high precision GPS observations. Chen et al. studied the variations of the low-degree gravity fields and showed that the variations were in good agreement with the loading effects modeled by land water, atmosphere and ocean models[3]. By using the ground- and space-based hydrological and meteorological observations as constraints to theoretically model the land surface states, the land water storage models can be obtained[4,5]. However, in some areas, the formulated models have great uncertainties due to the lack of data. The launch of the GRACE gravity satellites makes it possible to determine the Earth's external grav-

Received August 21, 2008; accepted November 12, 2008; published online March 6, 2009
doi: 10.1007/s11434-009-0006-9
†Corresponding author (email: zjc@asch.whigg.ac.cn)
Supported by Knowledge Innovation of Chinese Academy of Sciences (Grant No. KZCX2-YW-133), National Natural Science Foundation of China (Grant Nos. 40730316 and 40574034) and Frontier Domain Item of Chinese Academy of Sciences

Citation: Zhou J C, Sun H P, Xu J Q. Validating global hydrological models by ground and space gravimetry. Chinese Sci Bull, 2009, 54(9): 1534-1542, doi: 10.1007/s11434-009-0006-9

ity field and its variations with unprecedented precision[6,7]. The variations of the global land water storage can be inversely estimated through the harmonic potential coefficients of the Earth's temporal gravity fields[8]. Due to the largely accumulated errors in the harmonic coefficients of high degrees, however, only the low degree gravity field can be accurately determined. Jekeli developed a smoothing function to obtain the mean value with a given spatial resolution[9], which has been widely used for the GRACE-inversed water distribution. By this approach, only a resolution of several hundred kilometers can be achieved for the GRACE-inversed water distribution. Consequently, only the land water storage and its variations on large spatial scale can now be accurately determined.

Crossley et al.[10] pointed out that high precision ground-based gravimetry can calibrate the gravity changes derived from the GRACE on ground and validate the reliability of GRACE gravimetry. Because the SG (Superconducting Gravimeter) has broad dynamic linear measure range, high precision of 10^{-10} m s^{-2} and low drift rate of 10^{-8} m s^{-2} a^{-1} and high stability, it can detect the gravity changes on time scale from several seconds to several years and make it possible to monitor tiny signals induced by geodynamics[11,12]. As a result, the GGP (Global Geodynamic Project) was founded by the group of the SEDI, IUGG (Studies of Earth's Deep Interior, International Union of Geodesy and Geophysics)[13]. This project started in July, 1997. It is based on globally-distributed SGs manufactured by GWR company. In the SGs, there are identical central sensors and identical data filters and data gathering systems and identical sampling rates. The same data processing technique and analysis method are recommended by the GGP to obtain the tidal parameters in different frequency bands and to avoid artificial or technique-induced errors.

This project benefits us to investigate geodynamic phenomena on large spatial scale as well as regional or local gravity changes. With the accumulation of SG data, the long-term gravity changes due to variations of land water storage are at present feasible to be investigated. Boy et al. studied the seasonal gravity changes and showed that, after removal of tides and polar motion effects and atmosphere and nontidal ocean loading from observations, the residuals are highly correlated to the land water loading on seasonal time scale[14]. A similar conclusion was also drawn by Sato et al.[15]. Neumeyer et al. also calculated the effects of land water loading on gravity using harmonic expansion method and investigated the difference between the results derived from different hydrological models [16]. They showed that the fact that there is significant discrepancy in current hydrological models and the gravity observations could provide constraint to the hydrological model[16]. As a result, combination of the ground- and space-based gravity observations will be one resource to be used to validate the reliability of the global hydrological model.

At present, using temporal gravity variations derived from the GRACE as well as from 7 SGs and air pressure observations at GGP stations and global hydrological models and nontidal ocean model, the relation between residuals and land water loading is investigated to validate the reliabilities of the global hydrological models. In the investigation, only the gravity changes induced by land water are remained, other effects such as tides, atmosphere and nontidal ocean loading and polar motion are removed.

1 Processing of ground-based gravity observations

The information of the observations at 7 stations is listed in Table 1. The preprocessing on the original observations is carried out by Tsoft software, which includes removing the wrong data such as spikes, steps and gaps

Table 1 Information of SG observations

Station/country	Time band of data	Standard deviation (10^{-9} m s^{-2})	Atmosphere-gravity admittance (10^{-11} m s^{-2} Pa^{-1})
Wetzell/Germany	2000-01-01—2005-06-30	0.693	–1.78
Vienna/Austria	1998-01-01—2004-12-31	0.559	–2.76
Canberra/Australia	1998-01-01—2004-12-31	0.996	–3.09
Medicina/Italy	1998-01-01—2005-06-30	0.799	–2.65
Membach/Belgium	1998-01-01—2005-06-17	0.890	–2.78
Sutherland/South Africa	2000-10-23—2005-01-01	0.950	–2.38
Tigo/Chile	2002-12-05—2005-05-30	1.181	–2.65

and modifying the observations using remove-restore technique to obtain time series with disturbances removed and filtering the observations from minutely-sampled series to hourly-sampled ones[17].

The observations consist of tides y_{tide} as well as nontidal signal $N(t)$ and background noise $\varepsilon(t)$ and drift $d(t)$, which can be represented by[18]

$$y_{\mathrm{obs}}(t) = y_{\mathrm{tide}}(t) + N(t) + d(t) + \varepsilon(t), \qquad (1)$$

where $N(t)$ is mainly comprised of meteorological and hydrological effects and polar motion effects. The tides y_{tide} can be represented by

$$y_{\mathrm{tide}} = \sum_i \delta_i \sum_j A_j \cos(\omega_j t + \phi_j + \varphi_i), \qquad (2)$$

where i, j are tidal group index and tidal constituent index in corresponding tidal group, respectively. A_j, ω_j, ϕ_j are amplitude, angular frequency and initial phase of one constituent, respectively, and δ_i, φ_i are the amplitude factor and phase lead of one tidal group, respectively. From the hourly-sampled series, the equation group can be constructed through eq. (1). And through solving this equation group by least square method, the tidal parameter can be obtained. At present, the international standard harmonic analysis software of ETERNA is used to obtain the tidal parameters and error estimations[19].

To investigate the land water loading in gravity changes, the other signals should be removed. First, the tides are removed using synthetic tides which are constructed by amplitude factor and phase lead obtained by harmonic analysis through eq. (2). Comparing with the theoretical Earth's tides, using the synthetic tides has some advantages. For example, it can better remove the diurnal and semi-diurnal tides which have dominant energy in tides. Moreover, the ocean tide loading has the same frequency as the Earth's tides, which is one part of the synthetic tides. Therefore, the ocean tide loading needs not being removed individually. In addition, the gravity changes due to Earth's rotation changes are removed. As we know, the changes of Earth's rotation (polar motion and changes of length of day) will result in the centrifugal potential variation and consequently the gravity variation. The previous studies show that the high precision SG observations could obviously detect the gravity changes induced by polar motion[20−22]. Wahr once put forward an equation in calculating the gravity changes induced by polar motion (in unit of 10^{-8} m s^{-2})[20]:

$$\delta g(\theta, \lambda) = -3.9 \times 10^6 \sin 2\theta (m_1 \cos\lambda + m_2 \sin\lambda), \qquad (3)$$

in which θ and λ are co-latitude and longitude of the station of interest, respectively, m_1 and m_2 are two parameters representing polar motion. It is noted that m_1 orients to 0 meridian and m_2 orients to 90°E meridian. The effects of changes of length of day could be neglected because they are two orders in magnitude smaller than those of polar motion[20]. The changes of Earth's rotation result in the changes not only of gravity but also of ocean. Like ocean tides, the ocean surface changes due to polar motion also induce gravity changes. However, recent studies show that the observed amplitude factor of gravity induced by polar motion is about 1.18 and the difference from the theoretical value of 1.16 was caused by ocean polar tides[23]. This shows that the difference is about 2%. The gravity changes induced by polar motion are about 100×10^{-9} m s^{-2} in magnitude. Therefore, the difference in gravity is about 2×10^{-9} m s^{-2}. This effect is also much smaller than the effect of polar motion and consequently it could be neglected. That is to say, eq. (3) holds at present.

2 Seasonal change of gravity

After removing the synthetic tides and polar motion induced gravity, the residuals have obvious seasonal changes (see Figure 1), which mainly consist of annual and semi-annual variations. They are caused by global mass transportation, especially by the annual and semi-annual variations of the global cycle of atmosphere and ocean and land water.

The previous studies showed that, after removal of synthetic tides and gravity induced by polar motion, the negative correlation between residuals (downward positive) and air pressure changes at station was obvious. Therefore the local air pressure at station can be used to carry out atmosphere loading correction. Boy et al. showed that the difference between corrections using global air pressure model and using local air pressure was small[24]. Hence, the air pressure at station is used to correct atmosphere loading here. The atmosphere-gravity admittances for the stations are listed in Table 1.

Nontidal ocean loading effects are large over coastal areas while the effects in inland area are very small.

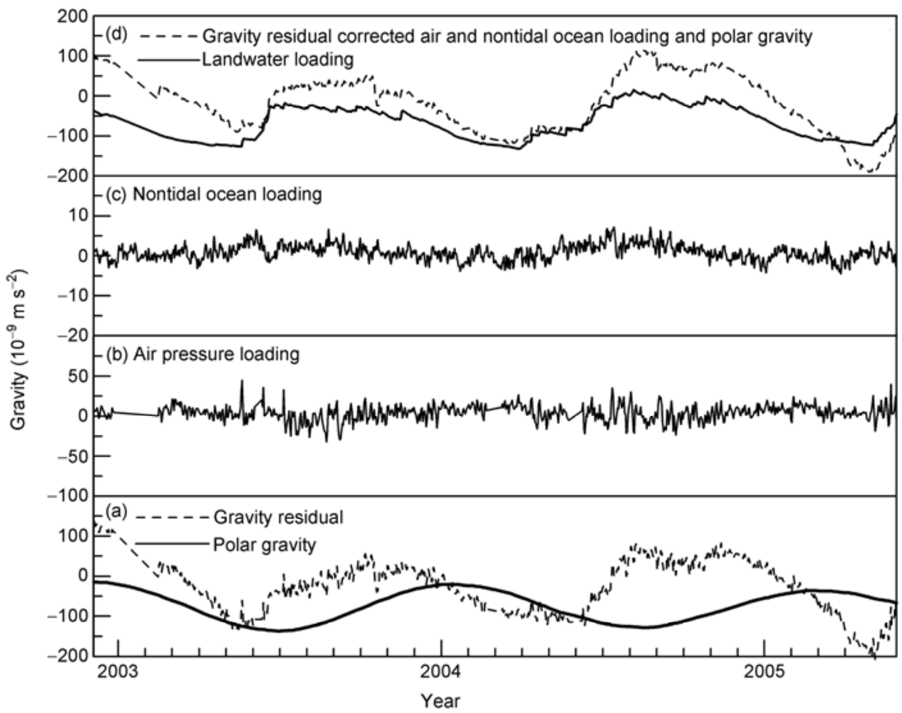

Figure 1 The processing and corrections on observations at station Tigo.

Figure 1 provides the effects of nontidal ocean loading on gravity at coastal station of Tigo. The effects are estimated by loading theory developed by Farrell[25]. In calculations, ocean bottom pressure data, which directly represent the load acting on ocean bottom, are transferred to equivalent water height through

$$h = \frac{P}{\rho g}, \tag{4}$$

in which g is the gravity acceleration at ocean bottom, taken the value 9.8 m s^{-2}, ρ is the density of sea water. From the convolution between Green's function and water height

$$Lg(\theta,\lambda) = R^2 \rho \iint_S G(\psi) h(\theta',\lambda') \sin\theta' \mathrm{d}\theta' \mathrm{d}\lambda', \tag{5}$$

the effects of nontidal ocean loading can be estimated. In eq. (5), R is the Earth's mean radius, θ',λ' are co-latitude and longitude of the grid point, ψ is angular distance from grid point to station, and S is ocean area. The Green's function has the form

$$G(\psi) = \frac{f}{R^2} \sum_{n=0}^{\infty} \{-n + (n+1)k_n' - 2h_n'\} P_n(\cos\psi), \tag{6}$$

where f is gravitational constant and P_n is Legendre polynomial. The ocean bottom pressure data come from ECCO (Estimating the Circulation and Climate of the Ocean, http://ecco.jpl.nasa.gov), which are globally distributed with latitude range from 79.5°S to 79.5°N. The spatial resolutions are from 1°×1° in polar area to 0.3°×0.3° in the equator. The data are interpolated to 1°×1° grid in calculations, and the temporal resolution is 12 hours.

After the atmosphere and nontidal ocean loading effects are removed, the residuals are mainly comprised of land water loading effects. Hence, through comparing residuals with the gravity changes calculated by the hydrological model, the reliability of the hydrological model can be validated. At present, the effects of land water loading are estimated by the same method as the one for nontidal ocean loading estimation except for that the area of the integral S is continent.

In our study, two hydrological models are used. The models give the equivalent water height. LaD (Land Dynamics) was constructed in terms of water balance and energy balance and assimilation of varieties of observations which are used as constraints to model. The observations include shortwave and longwave radiations, total precipitation, surface pressure, near-surface atmospheric temperature, humidity and wind speed. The spatial and time resolutions of this model are 1°×1° and 1 month, respectively[4]. GLDAS (Global Land Data Assimilation Systems) made use of the new generation of ground- and space- based observation systems, which provided data to constrain modeled land surface states. Constraints were applied in two ways. First, by forcing the land surface models with observation-based meteorological fields, biases in atmospheric model-based forcing can be avoided. Secondly, by employing data assimilation techniques, observations of land surface states can be used to constrain unrealistic model states. The spatial and time resolutions of this model are 1°×1° and 1 day respectively[5]. Land water is the sum of ground water and soil moisture and snow. When using these two models, the Antarctic and Greenland are excluded for difficulties in well estimating the water content under the secular ice sheets in these areas.

3 Reduction of GRACE satellite gravity

The variations of gravity field solved by GRACE satellites observations are represented by potential coefficients which are mainly contributed by mass change at Earth's surface and mass redistribution in Earth's interior due to surface mass loading. The Earth's tectonic movement also contributes the potential coefficients. On seasonal time scale, however, the variations of gravity field are dominantly induced by global land water changes based on the GRACE observations[16].

In the calculation of gravity variation induced by land water loading, the effects of loading-induced displacement are included, which are represented by the item of $-2h_n'$ in eq. (6). However, they are not included in the observations of GRACE satellites. Therefore, to compare the two results mentioned above with each other, this item is added to the GRACE results[16]. Let U be the change of direct gravitational potential induced by the change of water mass on the Earth's surface and W be the GRACE-derived gravity potential, then

$$\begin{aligned} W(r,\theta,\lambda) &= \sum_{n=0}^{n\mathrm{Max}} W_n = \sum_{n=0}^{n\mathrm{Max}} (1+k_n')U_n \\ &= \frac{fM}{R}\sum_{n=0}^{n\mathrm{Max}}\left(\frac{R}{r}\right)^{n+1}\sum_{m=0}^{n}[C_{nm}\cos(m\lambda) \\ &\quad + S_{nm}\sin(m\lambda)]\bar{P}_{nm}(\cos\theta), \end{aligned} \tag{7}$$

where r,θ,λ are spherical coordinates of station, M is the mass of Earth, and k_n' is load Love number corresponding to the additional potential induced by mass redistribution in the Earth's interior due to loading, $n\mathrm{Max}$ is the maximum degree of potential coefficients given by the GRACE-recovered gravity field, C_{nm}, S_{nm} are potential coefficients of sine and cosine parts with degree n and order m, $\bar{P}_{nm}$ is fully normalized associated Legendre function with degree n and order m, which satisfies the following condition:

$$\int_{-1}^{1}\left[\bar{P}_{nm}(x)\right]^2 \mathrm{d}x = 2(2-\delta_{m0}), \tag{8}$$

where δ_{ij} is Kronecker symbol. In terms of surface loading theory, if the gravitational potential of the loading mass is given, then the vertical displacement due to loading can be obtained. This displacement is the product of equilibrium tidal height and load Love number:

$$H_n = h_n' \frac{U_n}{\gamma}, \tag{9}$$

where γ is the gravity at station, and h_n' is load Love number corresponding to vertical displacement. Then the formula in calculating the gravity on Earth's surface from gravity potential can be obtained as

$$\begin{aligned} \Delta g(\theta,\lambda) &= \frac{fM}{R^2}\sum_{n=0}^{n\mathrm{Max}}\left(n+1-\frac{2h_n'}{1+k_n'}\right) \\ &\sum_{m=0}^{n}\left[C_{nm}\cos(m\lambda)+S_{nm}\sin(m\lambda)\right]\bar{P}_{nm}(\cos\theta). \end{aligned} \tag{10}$$

Now the results from eq. (10) are comparable with land water loading gravity or ground-based observations.

The difference between eq. (10) and the corresponding equation given by ref. [16] is that the denominator of displacement item in eq. (10) is $1+k_n'$ while it is 1 in ref. [16]. At present, the item is derived in terms of the definition of load Love number in which the vertical displacement is the product of load Love number and equilibrium tidal height. However, in ref. [16], it was derived in terms of the gravity potential in which the vertical displacement is the product of load Love number and geoidal height. Although the numerical results show that the difference is not obvious, the eq. (10) at present is more religious than that given in ref. [16].

In the calculation of gravity from gravity potential coefficients, 600 km smoothing radius is used in Gaussian smoothing function[9,26]. And correspondingly, the harmonic degree is truncated at 30. The monthly mean gravity fields recovered by GRACE are provided by GFZ (http://isdc.gfz-potsdam.de)[27].

4 Numerical results and discussions

As an example, the processing and analysis on observations at station Tigo are discussed in detail first. In Figure 1(a), the dash line means residuals after removing synthetic tides from observations. The magnitude of these residuals is about 400×10^{-9} m s^{-2}. The solid line in figure 1a means the gravity changes induced by polar motion. The magnitude of the changes is about 100×10^{-9} m s^{-2}. From the first half of the time band, there is a good agreement with each other in phase. This shows that the gravity changes induced by polar motion are distinguishable in high precision gravity observations. Figure 1(b) shows the gravity changes induced by atmosphere loading. At station Tigo, the air pressure variations are about 29×10^{2} Pa in magnitude and correspondingly the gravity variations are about 80×10^{-9} m s^{-2} derived through the admittance. Figure 1(c) gives the gravity variations induced by nontidal ocean loading with magnitude of about 10×10^{-9} m s^{-2}. Because station Tigo is located in coastal area, the loading effects will be much smaller than this value for inland stations. In Figure 1(d), the solid line represents the gravity variations induced by land water loading calculated from the hydrological model of GLDAS. The magnitude of these variations is about 150×10^{-9} m s^{-2}. The dash line in Figure 1(d) means the residuals after removing the effects of polar motion and atmosphere and nontidal ocean loading from the residuals in Figure 1(a). Comparing the two lines in Figure 1(d) with each other, it shows that the residuals and the land water loading effects have strong correlation of 0.85, which indicates that the seasonal variations of ground-based observations are contributed by local water cycle. However, there is discrepancy in magnitude. This difference is mainly caused by uncertainty in hydrological model and errors in observations and some unidentified geodynamic and tectonic processes. The numerical test shows that the loading effects estimated only from the land water storage among the area around the station with radius of 100 km can reach 80% of the total loading effects. To reach 95%, the radius of 250 km is needed[28].

Therefore, after filtering the seasonal variations out from the long-term continuous ground-based gravity observations and efficiently correcting global or local atmosphere loading effects, the residuals may useful to inverse local land water storage variations. This will provide a reliable way to monitor and investigate the local land water storage variations.

By the same stages, the observations at other stations are processed. Similarly, Figure 2 gives the same results as in Figure 1(d) except for that the hydrological model used here is LaD. For station Membach, in the second halves of years 2000 and 2002, there are obvious discrepancies between land water loading effects and residuals. While in other time bands, the two series are in good agreement with each other not only in magnitude but also in phase. For station Wettzell, the agreement is quite obvious between the two series, especially in magnitude. This shows that the observed seasonal variations of gravity are caused by the water cycle. Additionally, from Figure 2, the observed gravity variations lag those calculated from hydrological model by 26 days. This phenomenon has been also found in station Wuhan[28]. For station Sutherland located in coastal area in south-Africa, on seasonal time scale, the agreement between land water loading effects and residuals is also obvious with some exceptions in special time bands such as Apr. through Jun. in 2003. For station Vienna, the good agreements in magnitude and phase also exist. Like station Sutherland, for coastal station Canberra, the agreement on seasonal time scale is also distinguishable. At Medicina, the SG-obseved results agree well with the LaD-derived results in phase while the former differs from the latter in magnitude. This implies that, due to low spatial resolution of 1°×1° of hydrological model, the gravity variations induced by land water loading are regional mean values and are not accurate enough to interpret gravity changes by the local environmental factors at this station. Therefore, the model is ought to be refined later. This also provides us with an idea to constrain hydrological model with gravity observations.

As a whole, the residuals of gravity observations agree well with the gravity variation induced by land water loading, and the seasonal variations of gravity are contributed by globally large spatial scale water cycle. Nowadays, because the air pressure and ocean and land water models do not have high resolutions, and the environmental noise is difficult to be effectively modeled, there are difficulties in investigating high frequency signals in gravity residuals and local environmental effects. This needs to resort to constructions of accurate local models. Whereas, the meteorological and hydrological observations near stations will benefit to reliably

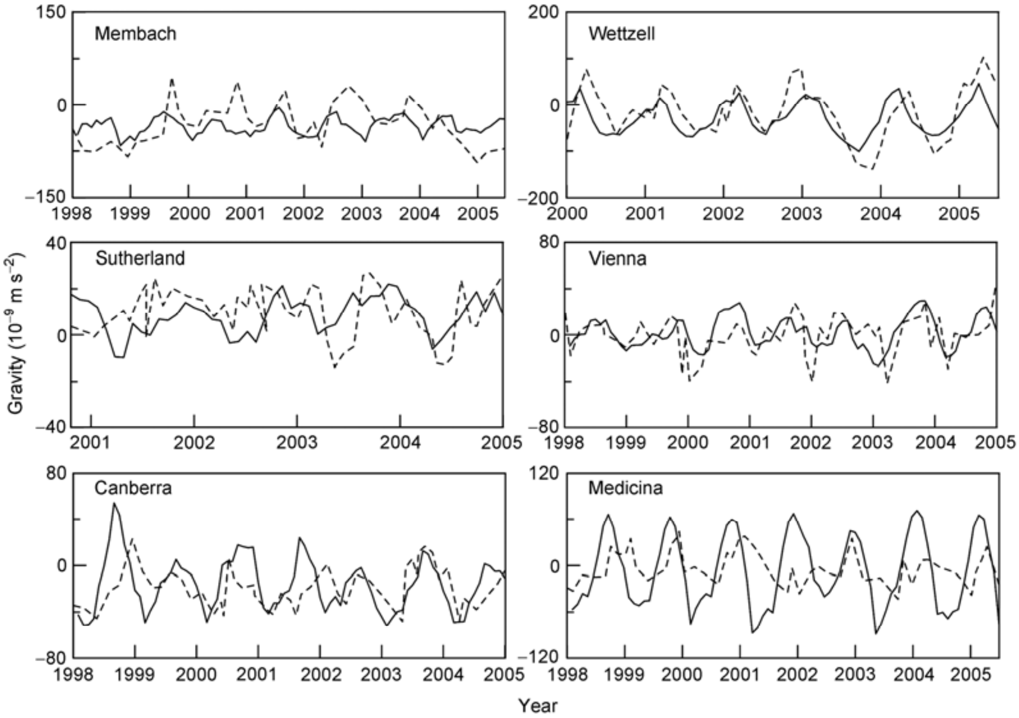

Figure 2 Comparison between gravity residuals (dash line) and the effects of land water loading on gravity (solid line).

interpret the observed gravity changes.

In order to compare the GRACE-derived results with the land water loading effects, the gravity variations at SG stations are calculated through eq. (10) using potential coefficients of gravity fields recovered by GRACE from Feb. 2003 to Jun. 2005, provided by GFZ. Since the gravity changes derived from the GRACE are mean values with smoothing radius of 600 km, in order to validate GRACE-derived results, the comparisons with SG results and land water loading effects calculated with LaD and GLDAS models are carried out, which are shown in Figure 3. The SG-observed results and GLDAS-derived results are monthly-averaged values. It is obvious that the GRACE-derived results agree well with the SG-observed results on seasonal time scale. Due to different spatial scales, however, there are discrepancies at some stations such as at Tigo in 2003 and at Sutherland in 2004 and at Wettzell in 2005.

The three kinds of results (GRACE, SG, land water loading) are in good agreement in 2003 and 2004. Especially at Membach, the agreement is very obvious. While in the first half of year 2005, the agreement is not good at some stations. For example, at Sutherland, the two results from hydrological models agree well with each other and differ from the GRACE-derived results. At Canberra, the GRACE-derived results agree well with the LaD-derived results while differ from the GLDAS-derived results. At Medicina, the results from hydrological models are obviously larger than the observed values. It should be noted that, at Vienna, the results both from the GRACE and SG and from hydrological models are in good agreement either in magnitude or in phase. This implies that the accuracies of the hydrological models around the stations are reliable.

The gravity changes derived from GRACE are smoothed means by a smoothing function with radius of 600 km, which reflect the effects of water mass migration in large region on gravity. Therefore, some local signals are impaired. On the contrary, SG-observed gravity variations include abundant local signals. The environmental effects with high frequency are filtered in the monthly mean of SG-observed gravity variations while those with low frequency are still remained. This means that GRACE-derived results are averaged values in time and space while the SG-observed results are averaged values in time. Hence, the difference between the two results is acceptable in special station. This difference is indeed due to local effects. However, it is not doubt that the precision of the SG is higher than that of the GRACE, which is also verified by Table 1. Therefore, after accurately correcting the local effects, the SG-observed results can calibrate the GRACE-derived results.

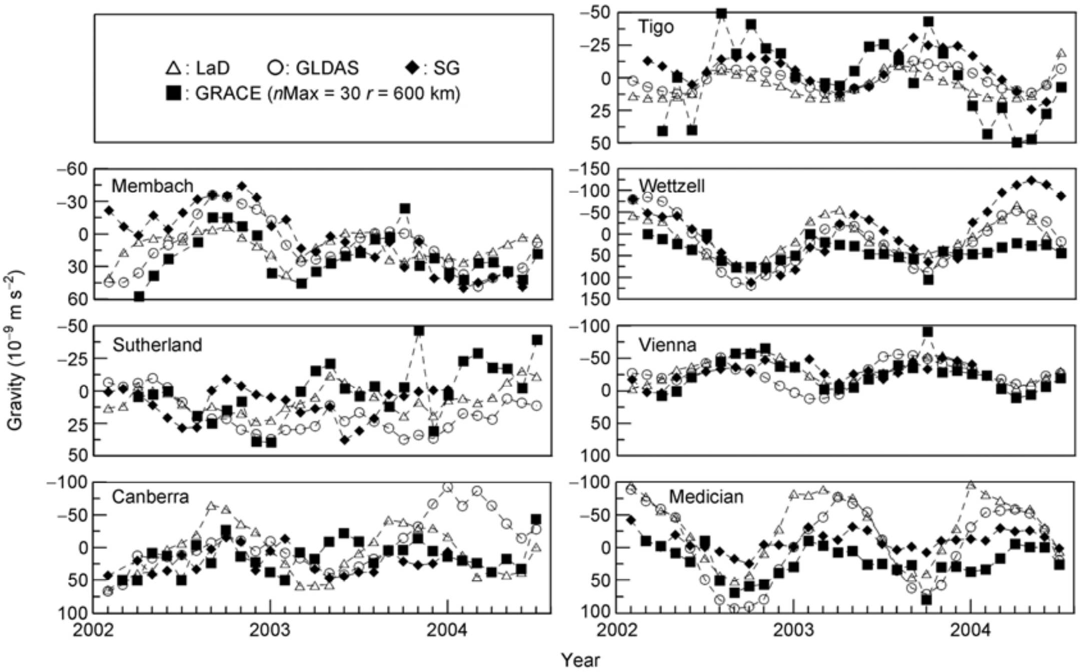

Figure 3 Comparison of results from SGs and GRACE and hydrological models.

5 Conclusion

Using SG observations as well as air pressure observations at 7 GGP stations and global hydrological models and nontidal ocean model, the seasonal variations of gravity are investigated. The results show that the variations are directly relevant to global water cycle, which contributes the gravity variations. Although the loading effects on gravity estimated by the models are different from the observations at special station due to the low spatial resolution of the models, as a whole, there are good agreements between the modeled and observed gravity variations. Therefore, the current hydrological models are applicable in investigations of geodesy and geophysics, especially in those investigations with large spatial scale. And the gravity observatory ought to be equipped with meteorological and hydrological measure facilities so that the gravity observations can be interpreted scientifically.

The comparisons between the gravity changes caused by the land water loading effects and those derived from GRACE show that the GRACE gravity measurements are efficient for monitoring seasonal variations of land water storage, while the local characteristic of gravity variations is not obvious due to large spatial scale. Nevertheless, combining the ability of inversing large spatial scale water transportation of GRACE and the ability of constraining local water transportation of ground-based gravity surveying will benefit to investigate regional water storage changes. The recently developed monitoring network of the tectonic environment in Chinese mainland is a network with high precision in gravity measurements. Combining the GOCE satellite gravity mission in the future, the network will play an important role in studies of the regional gravity fields and water storage changes.

1 Zhang F P, Dong D N, Cheng Z Y, et al. Crustal vertical seasonal variations in China observed by GPS (in Chinese). Chinese Sci Bull, 2002, 47(18): 1370−1377

2 Zhang S Y, Zhong M, Yan H M, et al. Meteorological excitation on annual variation of vertical displacement at Chinese GPS fundamental stations (in Chinese). Sci Surv Map, 2004, 29(2): 34−36

3 Chen J L, Wilson C R, Tapley B D. Interannual variability of low degree gravitational change, 1980−2002. J Geod, 2005, doi: 10.1007/s00190-004-0417-y[DOI]

4 Milly P C D, Shmakin A B. Global modeling of land water and energy balances. Part I: The land dynamics (LaD) model. J Hydromet, 2002, 3(3): 283−299[DOI]

5 Rodell M, Houser P R, Jambor U, et al. The global land data assimilation system. Bull Am met Soc, 2004, 85: 381−394[DOI]

6 Tapley B, Ries J, Bettadpur S, et al. GGM02-An improved Earth gravity field model from GRACE. J Geod, 2005, 79(8):

467－478[DOI]
7 Zhou X H, Hsu H, Wu B, et al. Earth's gravity field derived from GRACE satellite tracking data (in Chinese). Chin J Geophys, 2006, 49(3): 718－723
8 Ramillien G, Cazenave A, Brunau O. Global time variations of hydrological signals from GRACE Satellite gravimetry. Geophys J Int, 2004, 158: 813－826[DOI]
9 Jekeli C. Alternative methods to smooth the Earth's gravity field. Rep. 327, Dep Geod Sci and Surv, Ohio State Univ, Columbus, 1981
10 Crossley D, Hinderer J, Llubes M, et al. The potential of ground gravity measurements to validate GRACE data. Adv Geosci, 2005, 1: 1－7
11 Rosat S, Hinderer J, Crossley D, et al. The search for the Slichter mode: comparison of noise levels of superconducting gravimeters and investigation of a stacking method. Phys Earth Planet Inter, 2003, 140: 183－202[DOI]
12 Sun H P, Xu H Z. Execution and prospect for the global geodynamics project cooperation (in Chinese). Adv Earth Sci, 1997, 12(2): 152－157
13 Crossley D, Hinderer J, Casula G, et al. Network of superconducting gravimeters benefits a number of disciplines. EOS, 1999, 80(11): 121125－121126
14 Boy J P, Hinderer J. Study of the seasonal gravity signal in superconducting gravimeter data. J Geodyn, 2006, 41: 227－233[DOI]
15 Sato T, Boy J P, Tamura Y, et al. Gravity tide and seasonal gravity variation at Ny-Ålesund, Svalbard in Arctic. J Geodyn, 2006, 41: 234－241[DOI]
16 Neumeyer J, Barthelmes F, Dierks O, et al. Combination of temporal gravity variations resulting from superconducting gravimeter (SG) recordings, GRACE satellite observations and global hydrology models. J Geod, 2006, 79: 573－585[DOI]
17 Van Camp M, Vauterin P. Tsoft: graphical and interactive software for the analysis of time series and Earth tides. Comput Geosci, 2005, 31(5): 631－640 [DOI]
18 Chen X D, Sun H P. Comparison and investigation of the analysis techniques for tidal gravity observations. In: Zhu Y Z, Sun H P, eds. Progress in Geodesy and Geodynamics (in Chinese). Wuhan: Hubei Science & Technology Press, 2004. 364－370
19 Wenzel H G. The nanogal software: data processing package ETERNA 3.3. Bull Inf Marées Terrestres, 1996, 124: 9425－9439
20 Wahr J M. Deformation induced by polar motion. J Geophys Res, 1985, 90(B11): 9363－9368[DOI]
21 Xu J Q, Sun H P, Yang X F. A study of gravity variations caused by polar motion using superconducting gravimeter data from the GGP network. J Geod, 2004, 78(3): 201－209[DOI]
22 Yang X F, Sun H P, Xu J Q. Detection of gravitational effect of polar motion by use of auto-regression model (in Chinese). J Geod Geodyn, 2004, 24(2): 109－114
23 Ducarme B, Venedikov A P, Arnoso J, et al. Global analysis of the GGP superconducting gravimeters network for the estimation of the pole tide gravimetric amplitude factor. J Geodyn, 2006, 41: 334－344[DOI]
24 Boy J P, Gegout P, Hinderer J. Reduction of surface gravity data from global atmospheric pressure loading. Geophys J Int, 2002, 149: 534－545[DOI]
25 Farrell W E. Deformation of the Earth by surface loads. Rev Geophys Space Phys, 1972, 10: 761－797[DOI]
26 Whar J, Molenaar M, Bryan F. Time variability of the earth's gravity field: Hydrological and oceanic effects and their possible detection using GRACE. J Geophys Res, 1998, 103(B12): 30205－30229[DOI]
27 Flechter F. GFZ level-2 processing standards document. GRACE 327－743, http://isdc.gfz-potsdam.de
28 Xu J Q, Zhou J C, Luo S C, et al. Study on characteristics of long-term gravity changes at Wuhan station. Chinese Sci Bull, 2008, 53(13): 2033－2040[DOI]